Dissipative Energization of Baroclinic Waves by Surface Ekman Pumping

SUKYOUNG LEE

Department of Meteorology, The Pennsylvania State University, University Park, Pennsylvania

(Manuscript received 24 August 2009, in final form 25 February 2010)

ABSTRACT

A two-layer quasigeostrophic model is used to study the effect of lower boundary Ekman pumping on the energetics of baroclinic waves. Although the *direct* impact of the Ekman pumping is to damp the total eddy energy, either the eddy available potential energy (EAPE) or the eddy kinetic energy (EKE), individually, can grow because of the Ekman pumping. Growth of EAPE is favored if the phase difference between the upper and lower wave fields is less than a quarter wavelength, and EKE is favored if the phase difference is greater than a quarter wavelength. A numerical model calculation shows that the EAPE growth occurs directly through the Ekman pumping and that the increased EAPE can in turn lead to further growth by strengthening the baroclinic energy conversion from zonal available potential energy to the EAPE. Through this *indirect* effect, the Ekman pumping can increase the net production of total eddy energy.

1. Introduction

In the context of the two-layer quasigeostrophic (QG) model, it has been known for almost five decades that Ekman pumping, if present only at the lower boundary, can destabilize baroclinic waves. For example, Holopainen (1961) performed a linear stability analysis of the two-layer model and found that the lower boundary Ekman pumping broadens the marginally stable curve of the inviscid flow so as to destabilize both longer and shorter zonal waves. Essentially the same result was found by Pedlosky (1983), and also by Weng and Barcilon (1991), who used a linear Eady-like model (Eady 1949). Pedlosky (1983) further showed, with a weakly nonlinear analysis, that while the destabilized wave can grow initially, as the wave changes the mean flow the wave eventually decays. The final result is zero wave amplitude with an altered mean flow.

Nonlinear numerical model calculations also found that lower-layer Ekman damping can energize baroclinic waves. In their study of QG turbulence with a doubly periodic two-layer model, Hua and Haidvogel (1986) found that lower-layer Ekman pumping acts as a source of energy for the baroclinic waves. This finding was supported by Rivière et al. (2004), who used a primitive equation model to study effect of bottom friction on baroclinic eddies in an oceanic jet. Using a two-layer QG model, Lee (2010) showed that surface Ekman pumping acting directly on the eddies can increase eddy potential enstrophy. Thompson and Young (2007) found that for β less than a critical value, the addition of bottom friction produces a heat flux that is weaker than the inviscid prediction by Held and Larichev (1996) and Lapeyre and Held (2003). However, for β larger than a critical value, the inclusion of bottom friction results in a heat flux that is stronger than the inviscid prediction. Although linear destabilization may be relevant for these nonlinear results, to distinguish between linear and nonlinear influences the nonlinear behavior will be referred to as ''dissipative energization'' and the linear instability as ''dissipative destabilization.''

The above nonlinear results suggest for the atmosphere that surface Ekman pumping may play a nontrivial role for the equilibration process of midlatitude baroclinic waves. In spite of the potentially important role of surface Ekman pumping, the physical process by which Ekman pumping can energize baroclinic waves is not well understood. Dissipative energization of baroclinic waves, found in various numerical models, has often been attributed to the barotropic governor mechanism (James and Gray 1986; James 1987). While this may indeed be the case, the mechanism to be presented in this study differs from the barotropic governor mechanism, for which surface friction influences

Corresponding author address: Sukyoung Lee, Department of Meteorology, The Pennsylvania State University, University Park, PA 16802.
E-mail: sl@meteo.psu.edu

DOI: 10.1175/2010JAS3295.1

the eddies through the horizontal shear of the zonal mean flow.

In this study, the results of Lee (2010) are further analyzed from the viewpoint of the Lorenz energy cycle (Lorenz 1955) to help us better understand the workings of the dissipative energization.

2. Model

The model used in this study is a standard two-layer QG channel model on a β plane, with equal layer depths and flat rigid boundaries on the top and the bottom. This model is identical to that used by Lee (2010), wherein the dimensionless governing potential vorticity (PV) equations are

$$\frac{\partial q_1}{\partial t} + J(\psi_1, q_1) = \kappa_T(\hat{\psi} - \hat{\psi}_e) - \nu\nabla^6\psi_1 \quad \text{and} \tag{1.1}$$

$$\frac{\partial q_2}{\partial t} + J(\psi_2, q_2) = -\kappa_T(\hat{\psi} - \hat{\psi}_e) - \kappa_M\nabla^2\psi_2 - \nu\nabla^6\psi_2, \tag{1.2}$$

where the potential vorticity q_j satisfies

$$q_j = \beta y + \nabla^2\psi_j + (-1)^j\hat{\psi}, \quad j = 1, 2. \tag{1.3}$$

The subscript $j = 1$ and 2 refers to the upper and lower layers, respectively, ψ_j is the streamfunction, and $\hat{\psi} \equiv (\psi_1 - \psi_2)/2$. The model is nondimensionalized by the Rossby radius of deformation λ_R for the horizontal length scale, by the vertical wind shear U for the velocity scale, and by λ_R/U for the time scale.

The model is driven toward a prescribed thickness field $\hat{\psi}_e \equiv (\psi_{e1} - \psi_{e2})/2$, which is analogous to the radiative equilibrium temperature field. For simplicity, it is assumed that $u_{e2} \equiv -\partial\psi_{e2}/\partial y = 0$ everywhere. The coefficients κ_T and κ_M are the thickness and Ekman damping rates, respectively. To emphasize its analogous role in the atmosphere, the thickness damping will be referred to hereafter as thermal damping. The term $\nu\nabla^6\psi_j$ represents the enstrophy cascade toward subgrid scales, and the value of ν determines the cascade rate.

3. Energetics

To derive the eddy kinetic energy (EKE) and eddy available potential energy (EAPE) separately, we start with the QG vorticity and the interfacial height equations. Ignoring the high-order diffusion terms, we have

$$\frac{\partial\zeta_1}{\partial t} + J[\psi_1, (f + \zeta_1)] = -f_oD_1, \tag{2.1}$$

$$\frac{\partial\zeta_2}{\partial t} + J[\psi_2, (f + \zeta_2)] = -f_oD_2, \quad \text{and} \tag{2.2}$$

$$\frac{\partial\eta}{\partial t} + J(\psi_2, \eta) = w_I - \kappa_T(\eta - \eta_E), \tag{2.3}$$

where the vorticity $\zeta_j = \partial v_j/\partial x - \partial u_j/\partial y$; the divergence $D_j = \partial u_j/\partial x + \partial v_j/\partial y$; $w_I = w(H + \eta)$, in which I represents the interface and H is the mean depth for each layer; and η is the interfacial height, which can be written as

$$\eta = -\frac{f}{g^*}(\psi_1 - \psi_2)/2. \tag{3}$$

In (3) $g^* = g[(\rho_2 - \rho_1)/2\rho_2]$, where ρ_j is the density.

Integrating the lower-layer continuity equation vertically, with the QG assumption $\eta \ll H$, yields

$$w_I - w(0) = -D_2H, \tag{4}$$

where the Ekman pumping velocity at the surface $w(0) = (\kappa_MH/f_o)\zeta_2$ (Charney and Eliassen 1949; Holopainen 1961). Because we assume that Ekman pumping is absent at the upper boundary, vertical integration of the upper layer continuity equation yields

$$w_I = D_1H. \tag{5}$$

Eliminating w_I from (4) and (5), we have

$$D_1H + D_2H = w(0). \tag{6}$$

Dividing the flow field into a zonal mean and perturbation from the zonal mean, the perturbation vorticity and interfacial height equations take the form of

$$\zeta_{1t} + U_1\zeta_{1x} + v_1(\beta - U_{1yy}) + J(\psi_1, \zeta_1) = -f_oD_1, \tag{7.1}$$

$$\zeta_{2t} + U_2\zeta_{2x} + v_2(\beta - U_{2yy}) + J(\psi_2, \zeta_2) = -f_oD_2, \quad \text{and} \tag{7.2}$$

$$\eta_t + U_2\eta_x + v_2\Lambda_y = w_1 - \kappa_T\eta, \tag{7.3}$$

where the lowercase variables now denote perturbations and the uppercase variables denote the zonal mean. Specifically, U_j and Λ denote the zonal-mean zonal wind and the zonal-mean interfacial displacement, respectively. The only exception is D_j, which represents the perturbation divergence field. The subscripts x, y, and t refer to partial derivatives.

To obtain the EKE, (7.1) is first multiplied by $-\psi_1$ and (7.2) by $-\psi_2$. After integrating these equations in both x and y, and adding the resulting two equations, the EKE equation takes the form of

$$\frac{1}{2}\left(\frac{\overline{\left|\vec{\nabla}\psi_1\right|^2}+\overline{\left|\vec{\nabla}\psi_2\right|^2}}{2}\right)_t$$

$$=-\frac{1}{2}\sum_{i=1}^{2}U_i\overline{v_i\zeta_i}+\frac{1}{2}\sum_{i=1}^{2}f_o\overline{D_i\psi_i} \tag{8.1}$$

$$=-\frac{1}{2}\sum_{i=1}^{2}U_i\overline{v_i\zeta_i}+f_o\left[-\overline{\hat{\psi}D_2}+\frac{1}{2}\overline{\psi_1\frac{w(0)}{H}}\right] \tag{8.2}$$

$$=\underbrace{-\frac{1}{2}\sum_{i=1}^{2}U_i\overline{v_i\zeta_i}}_{\text{BT}}\quad\underbrace{-f_o\overline{\hat{\psi}D_2}}_{\text{C(EAPE,EKE)}}\quad\underbrace{+\frac{1}{2}\overline{\kappa_M\psi_1\nabla^2\psi_2}}_{\text{EKE}_{\text{Ek}}}, \tag{8.3}$$

where (6) is used to write (8.2) and the overbar denotes a zonal average. The first term on the rhs of (8.3), commonly referred to as the barotropic conversion (hereafter BT), represents the conversion from zonal kinetic energy (ZKE) to EKE, and the second term represents the conversion from EAPE to EKE. The third term represents the Ekman pumping contribution to the EKE (hence referred to as EKE_{Ek}).

The equation for EAPE can be obtained by multiplying (7.3) by $g^*\eta/H$. Using (3) and (4), the EAPE equation takes the form of

$$\frac{g^*}{H}\left(\frac{1}{2}\overline{\eta^2}\right)_t=\underbrace{-\frac{g^*}{H}\overline{v_2\eta}\Lambda_y}_{\text{BC}}\quad\underbrace{+f_o\overline{\hat{\psi}D_2}}_{-\text{C(EAPE,EKE)}}\quad\underbrace{-\kappa_M\overline{\hat{\psi}\nabla^2\psi_2}}_{\text{EAPE}_{\text{Ek}}}$$
$$-\kappa_T\frac{g^*}{H}\overline{\eta^2}. \tag{9}$$

The first term on the rhs of (9) is the conversion from zonal available potential energy (ZAPE) to EAPE, commonly known as the baroclinic energy conversion term (hereafter BC), the second term is the energy conversion from EAPE to EKE, the third term is the Ekman pumping contribution to the EAPE, and the fourth term is the radiative damping of EAPE. By adding (8.3) and (9), the total eddy energy (TEE) equation can be obtained:

$$\frac{1}{2}\left(\frac{\overline{\left|\vec{\nabla}\psi_1\right|^2}+\overline{\left|\vec{\nabla}\psi_2\right|^2}}{2}+\frac{g^*}{H}\overline{\eta^2}\right)_t=-\frac{1}{2}\sum_{i=1}^{2}U_i\overline{v_i\zeta_i}-\frac{g^*}{H}\overline{v_2\eta}\Lambda_y\underbrace{-\frac{\kappa_M}{2}\overline{\left|\vec{\nabla}\psi_2\right|^2}}_{\text{TEE}_{\text{Ek}}}-\kappa_T\frac{g^*}{H}\overline{\eta^2}. \tag{10}$$

The direct contribution of the Ekman damping to the TEE (TEE_{Ek}) is always negative. However, for EKE and EAPE individually, the Ekman pumping can contribute toward growth. As will be explained shortly, the latter property is central to the operation of the dissipative energization.

The Ekman pumping can contribute to EKE growth if the term EKE_{Ek} in (8.3) is positive. It can be seen, after integrating by parts, that EKE_{Ek} is positive if $\vec{\nabla}\psi_1\cdot\vec{\nabla}\psi_2<0$. If the horizontal scales of ψ_1 and ψ_2 are equal, this inequality holds if ψ_1 and ψ_2 are negatively correlated, which corresponds to a phase difference between ψ_1 and ψ_2 that satisfies $\pi/2<\delta\phi<3\pi/2$. This result is slightly different from that of Holopainen (1961). In his two-level model, the Ekman pumping velocity depends not only on ψ_2 but also on ψ_1.

Similarly, Ekman pumping can contribute toward EAPE growth if $\text{EAPE}_{\text{Ek}}>0$, that is, if $\vec{\nabla}\psi_1\cdot\vec{\nabla}\psi_2-|\vec{\nabla}\psi_2|^2>0$. Again assuming that the horizontal scales of ψ_1 and ψ_2 are equal, this inequality is satisfied if ψ_1 and ψ_2 are positively correlated, which implies that $|\delta\phi|<\pi/2$.

Figure 1 illustrates schema for the mechanism by which EKE and EAPE can grow through the Ekman pumping. Here, it is assumed that $|\psi_1|>|\psi_2|$. For the EAPE, η in this two-layer model is equivalent to temperature in a continuous model, with upward displacement ($\eta>0$) corresponding to cold air and downward displacement ($\eta<0$) to warm air. The solid curve in Fig. 1 denotes an initial η field, and the dashed curve indicates η after being subjected to Ekman pumping. If ψ_1 and ψ_2 are out of phase, the surface Ekman pumping can help convert the EAPE to EKE because it reduces $|\eta|$ (Fig. 1a). Similarly, if ψ_1 and ψ_2 are in phase, the surface Ekman pumping can generate EAPE, since it enhances $|\eta|$ (Fig. 1b).

Given that the direct impact of the Ekman pumping on the TEE is always dissipative (i.e., $\text{TEE}_{\text{Ek}}<0$), the observation that dissipative energization can occur implies that there must be an *indirect* influence through which Ekman pumping can increase TEE. From the Lorenz energy cycle, which in Fig. 2 flows in a counterclockwise direction, waves can grow via this indirect effect only if $\text{EAPE}_{\text{Ek}}>0$. This is because a positive EAPE_{Ek} can increase $|\eta|$, which in turn can promote an energy conversion (BC) from ZAPE to EAPE. This process is indicated schematically with the black arrows in Fig. 2 and will be referred to as the BC_{Ek} growth.

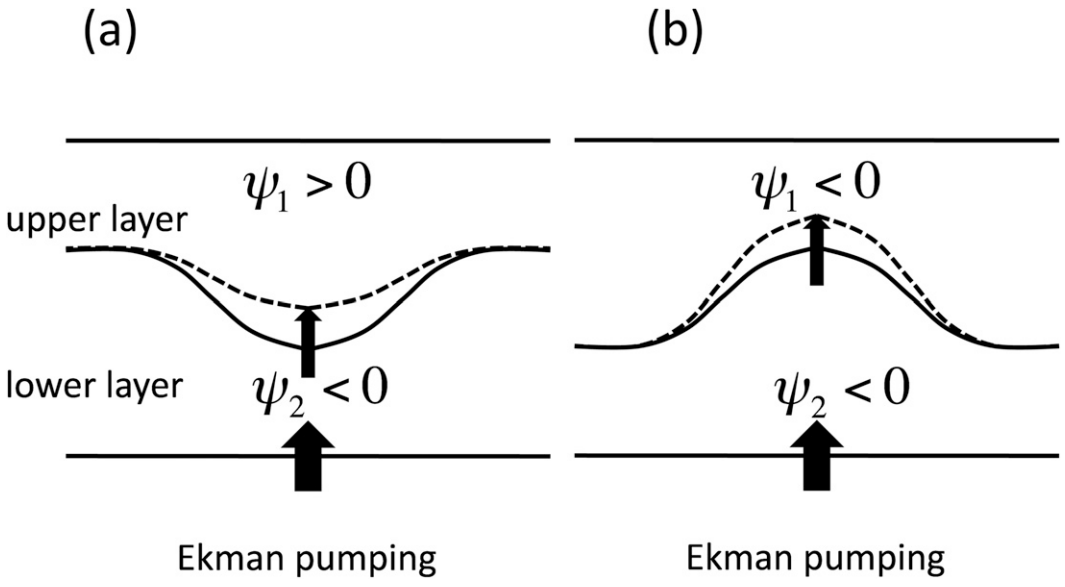

FIG. 1. Schema of (a) EKE and (b) EAPE production by surface Ekman pumping. In both frames, the wavy solid curve indicates the initial interface between the upper and lower layers for an inviscid fluid, and the dashed curve indicates the interface after the influence of the Ekman pumping takes place. It can be seen in (a) that the Ekman pumping helps convert EAPE to EKE, while in (b) the Ekman pumping generates EAPE by raising the interface.

If EKE_{Ek} is positive (Fig. 1a), which results in an increase in $|v_i|$, then BC can also increase in response. However, because an increase in $|v_i|$ also enhances BT, compared with the BC_{Ek} growth, this is an inefficient route toward dissipative energization. Holopainen (1961) provided a physical explanation for linear dissipative destabilization in terms of his version of EKE_{Ek} being positive. However, the above analysis for $EAPE_{Ek}$ suggests an alternative interpretation.

The barotropic governor mechanism of James and Gray (1986) and the self-maintaining jet mechanism of Robinson (2006) are also included in Fig. 2. For the latter mechanism, as discussed in Robinson (2006), the eddy momentum flux convergence at the jet center enhances the vertical shear of the zonal-mean zonal wind beyond that of the radiative equilibrium state. Although not explicitly stated in that paper, in order for this to result in wave growth, surface friction must be stronger than radiative damping (Lee 2010). Energetically, this means that changes in the ZKE, with the help of surface Ekman pumping, can increase ZAPE. As such, there are at least three different ways that surface Ekman pumping can energize baroclinic eddies through their impact on the ZAPE to EAPE energy conversion.

4. Test of the BC_{Ek} growth

a. An overview from statistically steady states

To test the above hypothesis that the EAPE growth by $EAPE_{Ek}$ can further promote the conversion from ZAPE to EAPE, we first examine the dependency of $EAPE_{Ek}$ on κ_M. For this purpose, we perform the numerical model calculations, using the same model settings [see (1.1) and (1.2)] as in Lee (2010). The basic state consists of a jetlike upper-layer zonal wind profile:

$$U_{1e} = e^{-y^2/\sigma^2},$$

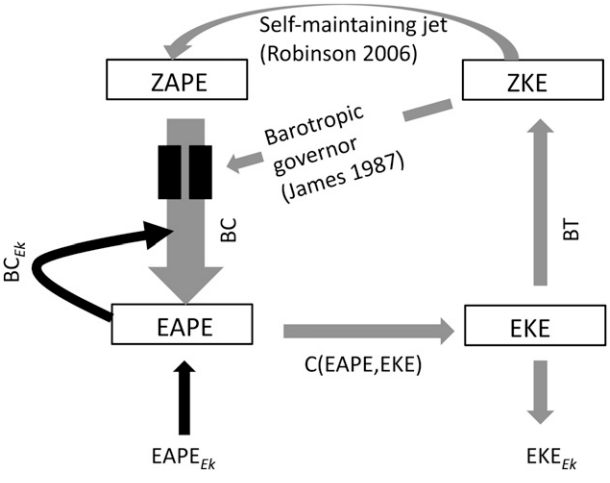

FIG. 2. Schema of the BC_{Ek} growth (black arrows) in the context of the Lorenz energy cycle. The direction of the arrows between the Ekman pumping and EAPE/EKE depends on $\delta\phi$. As a reference, the barotropic governor mechanism (James and Gray 1986; James 1987) is also shown, along with the self-maintaining jet mechanism (Robinson 2006). Following Fig. 1 of James (1987), the two black bars represent a damper that acts to weaken the energy conversion.

where $y = 0$ is at the middle of the channel and $\sigma^2 = 10$. The equilibrium lower-level wind U_{2e} is set to zero everywhere. For all simulations to be presented here, κ_T and ν are fixed at 30^{-1} and 5×10^{-4}, respectively. The width of the channel is 30, and there are 200 grid points across the channel. Figures 3a–d display time-mean values of $\mathrm{EAPE_{Ek}}$, along with that of other selected terms in (8.3) and (9), for different values of κ_M and β. To ensure that these values represent a statically steady state, the model was integrated for 2000 days, and the last 1000 days were used to calculate the time-mean values.

There are two noteworthy features from the simulations summarized in Fig. 3. First, for all nonzero values of β, $\mathrm{EAPE_{Ek}}$ first *increases* with κ_M, peaking either at $\kappa_M = 0.20$ (for $\beta = 0.15$) or at $\kappa_M = 0.30$ (for $\beta = 0.25$ and 0.30). Within the range $0.05 < \kappa_M < 0.2$, the fractional increase in $\mathrm{EAPE_{Ek}}$ is greater as β increases; the fractional increase is 58% for $\beta = 0.15$, 101% for $\beta = 0.25$, and 117% for $\beta = 0.30$. Second, for $\beta = 0.25$ and 0.30, where the fractional increase in $\mathrm{EAPE_{Ek}}$ is large, BC and EAPE also increase with κ_M. The above two features indicate that there is a range of optimal values of β and κ_M where the dissipative energization is more effective. While a direct comparison is impossible because of the differences in forcing, the dependency of BC on κ_M is consistent with the finding of Thompson and Young (2007). They found that for sufficiently large values of β, northward heat flux intensifies as their surface friction increases.

The above dependency on β is consistent with the interpretation of Lee (2010), who showed that dissipative amplification of eddy potential enstrophy hinges on the condition

$$\left|\frac{\partial Q_1}{\partial y}\right| \gg \left|\frac{\partial Q_2}{\partial y}\right|, \tag{11}$$

where Q_1 and Q_2 are the zonal mean PV in the upper and lower layer, respectively; under this condition, as long as the location of the extrema in the eddy PV flux and the zonal mean PV gradient coincide, eddy enstrophy generation is much greater in the upper layer than in the lower layer, leading to the condition $|q_1| \gg |q_2|$. In this case, because q_1 plays the dominant role in inducing both ψ_1 and ψ_2 (Bretherton 1966; Hoskins et al. 1985), $\delta\phi$ must be small. According to the argument pertaining to Fig. 1, all else being equal, smaller values of $\delta\phi$ coincide with greater $\mathrm{EAPE_{Ek}}$. Therefore, the dissipative energization would be favored under condition (11), which can more readily occur for larger values of β. Figures 3e–h show that the anticipated change in $\delta\phi$ with β is most evident for $\beta = 0.0$ and 0.15.

The dependency on κ_M is also consistent with the above interpretation that condition (11) favors a sufficiently small $\delta\phi$ and thus the dissipative energization. Figures 3e–h show that $\delta\phi$ monotonically increases with κ_M for all β, implying a weakening of the dissipative energization with κ_M. However, because the amplitude of $\mathrm{EAPE_{Ek}}$ is not only inversely proportional to $\delta\phi$ but also proportional to κ_M, there would be optimal, intermediate values of κ_M where maximum $\mathrm{EAPE_{Ek}}$ can be produced. As discussed above, Figs. 3a–d indeed show this behavior.

While this analysis provides a coherent interpretation for the dependency of $\mathrm{EAPE_{Ek}}$ and $\delta\phi$ on κ_M, the question still remains as to why $\delta\phi$ increases monotonically with κ_M. This increase in $\delta\phi$ is consistent with $(\partial Q_2/\partial y)(y = 0)$ becoming increasingly negative with κ_M (see Figs. 3e–h) while $(\partial Q_1/\partial y)(y = 0)$ remains essentially constant. [This can be inferred by the fact that $[(\partial Q_2/\partial y)/(\partial Q_1/\partial y)](y = 0)$ (see Figs. 3e–h) closely follows $\partial Q_2/\partial y$.] The only isolated exceptions occur for $(\beta, \kappa_M) = (0.0, 0.05)$ and $(0.0, 0.1)$. Because this simultaneous increase in $(|\partial Q_2/\partial y|/|\partial Q_1/\partial y|)(y = 0)$ and $\delta\phi$ with κ_M is consistent with condition (11), we interpret this increase in $\delta\phi$ as arising from $(\partial Q_2/\partial y)(y = 0)$ becoming increasingly negative with κ_M. This behavior can in turn be attributed to the Ekman damping effect on the zonal mean flow; as the damping strengthens, $-\partial^2 U_2/\partial y^2$, which is positive, would become smaller at the jet center. Because $\partial Q_2/\partial y \equiv \beta - \partial^2 U_2/\partial y^2 - (U_1 - U_2)/2$ the above change in $-\partial^2 U_2/\partial y^2$ would allow $(\partial Q_2/\partial y)(y = 0)$ to become increasingly negative as κ_M increases.

b. Transient evolutions

To test if $\mathrm{BC_{Ek}}$ growth can occur, it is necessary to examine the transient evolution of the energetics. We also ask how $\mathrm{BC_{Ek}}$ would differ between the regime where TEE increases with κ_M and that where TEE decreases with κ_M. Based on the results summarized in Fig. 3, we choose three cases: $(\beta, \kappa_M) = (0.25, 0.1)$, $(0.25, 0.2)$, and $(0.25, 0.5)$. The first case is where TEE increases with κ_M; the second case is where the TEE maximum occurs; the third case is where TEE decreases with κ_M. We choose the cases with $\beta = 0.25$ rather than $\beta = 0.30$ because most of the finite-amplitude states with $\beta = 0.30$ arise from subcritical instability (the arrows in Figs. 3a–d indicate the linear stability boundary). That is, the finite-amplitude states occur only when the model is initialized with finite-amplitude eddies (Lee and Held 1991). For this subcritical region, therefore, it is impossible to examine the initial transient evolution from the normal mode form.

For each of the three cases, the initial transient evolution is shown in Figs. 4a–c. For $\kappa_M = 0.1$ and 0.2, the initial spinup stage is followed by growth of the most unstable normal mode. (The spinup stage is not shown.) As can be inferred by the constant EAPE growth rates, the normal mode growth continues until day 100 for $\kappa_M = 0.1$, and until day 550 for $\kappa_M = 0.2$. In the latter

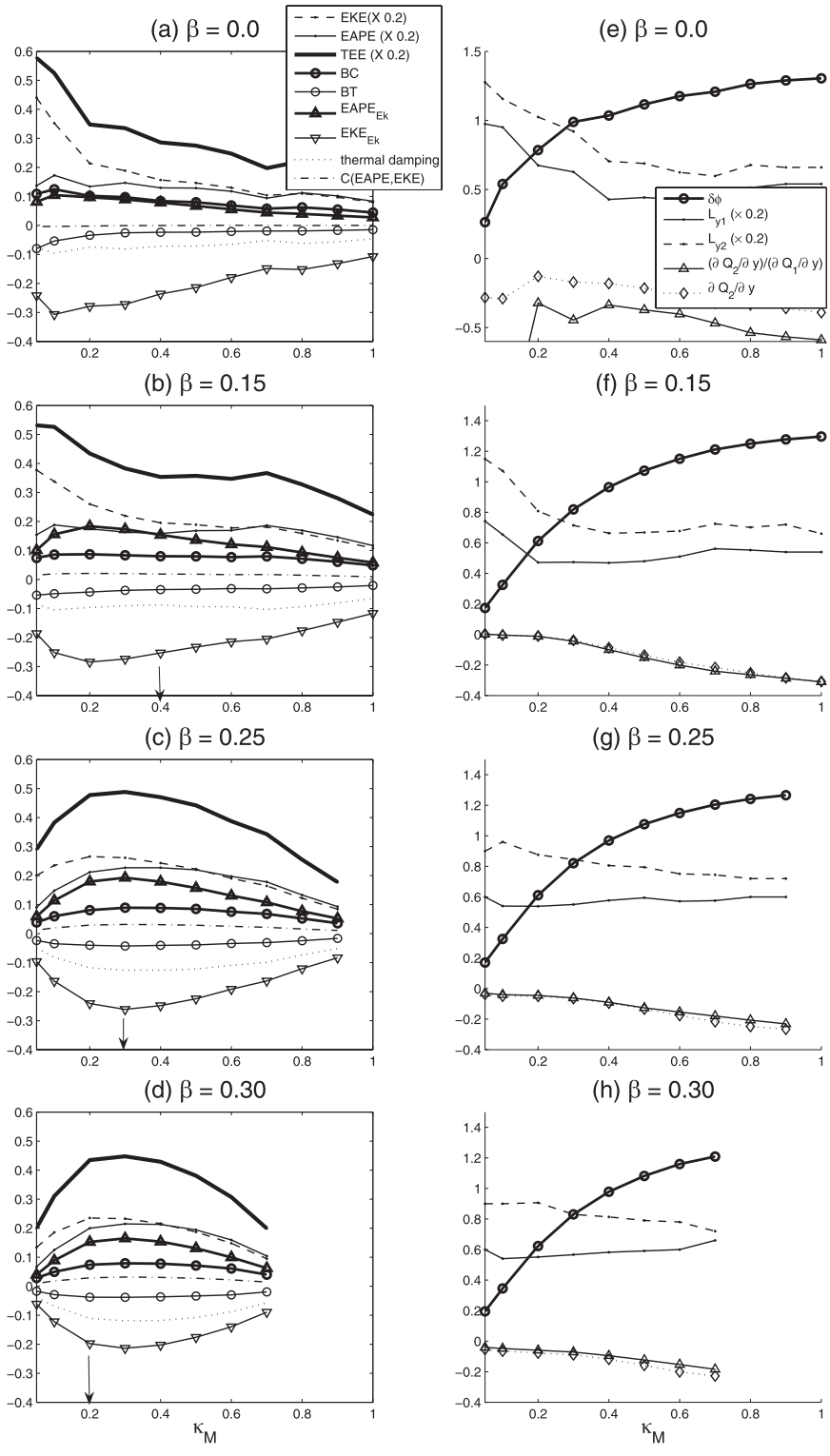

case, the linear growth stage is followed by a brief period (between days 550 and 750) of higher growth rates. Lee and Held (1991) interpreted this behavior in terms of a nonlinear growth ($\gamma > 0$) in the weakly nonlinear amplitude equation $\partial A/\partial t = \alpha A + \gamma|A|^2 A$ (Pedlosky 1970), where A is the wave amplitude. The finding in Lee (2010) suggests that this nonlinear growth may be due to the eddy-driven baroclinicity ("self-maintaining jet" mechanism; Robinson

2006). While this nonlinear growth is likely to foster the dissipative energization (Lee 2010), as will be explained below, the dissipative energization still occurs for $\kappa_M = 0.1$ where the nonlinear growth does not occur.

During the nonlinear growth period, the disturbance attains a finite amplitude, while sharply deviating from its normal mode form. The latter feature can be detected from the occurrence of a large change in the meridional scale and the vertical phase tilt of the wave field (see Figs. 4g,h). As can be seen, the deviation from normal mode form is characterized by a decrease in the meridional scale of the upper-layer eddy streamfunction L_{y1}, an increase in the meridional scale of the lower-layer eddy streamfunction L_{y2}, and a decrease in the vertical phase tilt $\delta\phi$. (The meridional eddy scales L_{y1} and L_{y2} were defined as the distance between the two points, on either side of the jet center, where the eddy streamfunction first changes sign.) The smallness in $\delta\phi$ implies that—as illustrated by Fig. 1—the EAPE can grow more effectively by the Ekman pumping. (In Figs. 4g–i, $1 - \mathrm{EAPE_{Ek}}$ is displayed to highlight the fact that the increase in $\mathrm{EAPE_{Ek}}$ is associated with the decrease in $\delta\phi$.) In fact, $\mathrm{EAPE_{Ek}}$, while smaller than BC initially, rapidly increases afterward; during the equilibrium stage $\mathrm{EAPE_{Ek}}$ is about twice as large as BC. This time evolution also demonstrates that the Ekman pumping–driven growth of EAPE is a nonlinear process and cannot be explained by the linear theory. As κ_M is increased from 0.2 to 0.5 (the initial state is day 1000 of the $\kappa_M = 0.2$ case), $\delta\phi$ rapidly increases (Fig. 4i), but $\mathrm{EAPE_{Ek}}$ still dominates over BC.

Having demonstrated that $\mathrm{EAPE_{Ek}}$ is the main contributor to the nonlinear growth of the eddy energy, we now test the hypothesis that the direct effect of the Ekman pumping can further enhance BC, and thus EAPE. To perform this test, we choose for the initial flow the model state at a time when $\mathrm{EAPE_{Ek}}$ attains a large value and integrate the model forward in time with $\kappa_M = 0.0$ in the eddy potential vorticity equation. In this integration, the zonal mean flow is still subject to the same Ekman damping so that the effect of the Ekman pumping on the eddies can be isolated from that on the zonal mean flow, as in the barotropic governor mechanism of James and Gray (1986) and James (1987). Although this model setting is unphysical, the initial behavior of the eddy energy can be used to test our hypothesis. For each of the three cases, with the model state indicated by the thick arrow (in Figs. 4a–c) as the initial state, the test run was performed and the resulting energetics over the next 50 model days are shown in Figs. 4d–f. For $\kappa_M = 0.5$, to test the sensitivity to the initial state, an additional calculation was performed using the model state indicated by the thin arrow (Fig. 4c) as the initial state. The result (not shown) is very similar to that shown in Fig. 4f.

For $\kappa_M = 0.1$, it can be seen that BC strengthens briefly, but it rapidly weakens during the next 10–15 days. The brief increase in BC can be understood as being due to the strengthening of the eddy meridional wind v_j, as evidenced by the rapid increase in the EKE, which is due to the zero $\mathrm{EKE_{Ek}}$. (As can be seen from Fig. 4a, $\mathrm{EKE_{Ek}}$ is the main sink of EKE when $\kappa_M \neq 0$.) In the face of this rapid EKE increase, the subsequent weakening in BC implies either that $|\eta|$ is becoming small or that the correlation between v_j and η has declined. Comparing the EAPE between Figs. 4a and 4d, it can be seen that $|\eta|$ of the test run is clearly smaller than that of the control run, even during the first five days when BC undergoes a strengthening. Because this decline in $|\eta|$ is due to $\mathrm{EAPE_{Ek}}$ being zero, we are led to conclude that the decline in BC (between days 3 and 18) is due to the absence of $\mathrm{EAPE_{Ek}}$ and its impact on BC (the black arrows in Fig. 2). The thermal damping is not found to play an important role here because the change in the thermal damping during the transient stage is small. In Fig. 4d, it is also interesting to observe that the initial EKE gain is followed by a slight reduction of EKE (between days 14 and 20). This EKE decline is consistent with the preceding reduction in C(EAPE, EKE), which closely follows BC. Beyond day 25, the EKE continues to increase, but again this is due to the zero $\mathrm{EKE_{Ek}}$. This long-time behavior is unphysical and therefore not meaningful.

As the value of κ_M increases (cf. Figs. 4d and 4e, and Figs. 4e and 4f), the initial period of BC strengthening becomes longer, and the subsequent decline of BC becomes smaller. In accordance with the earlier interpretation, this lengthening of the initial period is consistent with the more rapid EKE increase, and the smaller BC

←

FIG. 3. (a)–(d) The statistically steady state (average over days 1001–2000) of EKE, EAPE, baroclinic energy conversion, barotropic energy conversion, $\mathrm{EKE_{Ek}}$, $\mathrm{EAPE_{Ek}}$, thermal damping, and C(EAPE, EKE) for (a) $\beta = 0.0$, (b) $\beta = 0.15$, (c) $\beta = 0.25$, and (d) $\beta = 0.3$. In each case, the arrow indicates the stability boundary (to an accuracy of $\kappa_M = 0.1$). For the subcritical cases, the initial state is the final state of the case whose κ_M value is smaller by 0.1. (e)–(i) Statistically steady-state values for $\delta\phi$, $\partial Q_2/\partial y$, $(\partial Q_2/\partial y)/(\partial Q_1/\partial y)$, and L_{y1} and L_{y2}. The legend in (a) applies to (b)–(d), and that in (e) applies to (f)–(i).

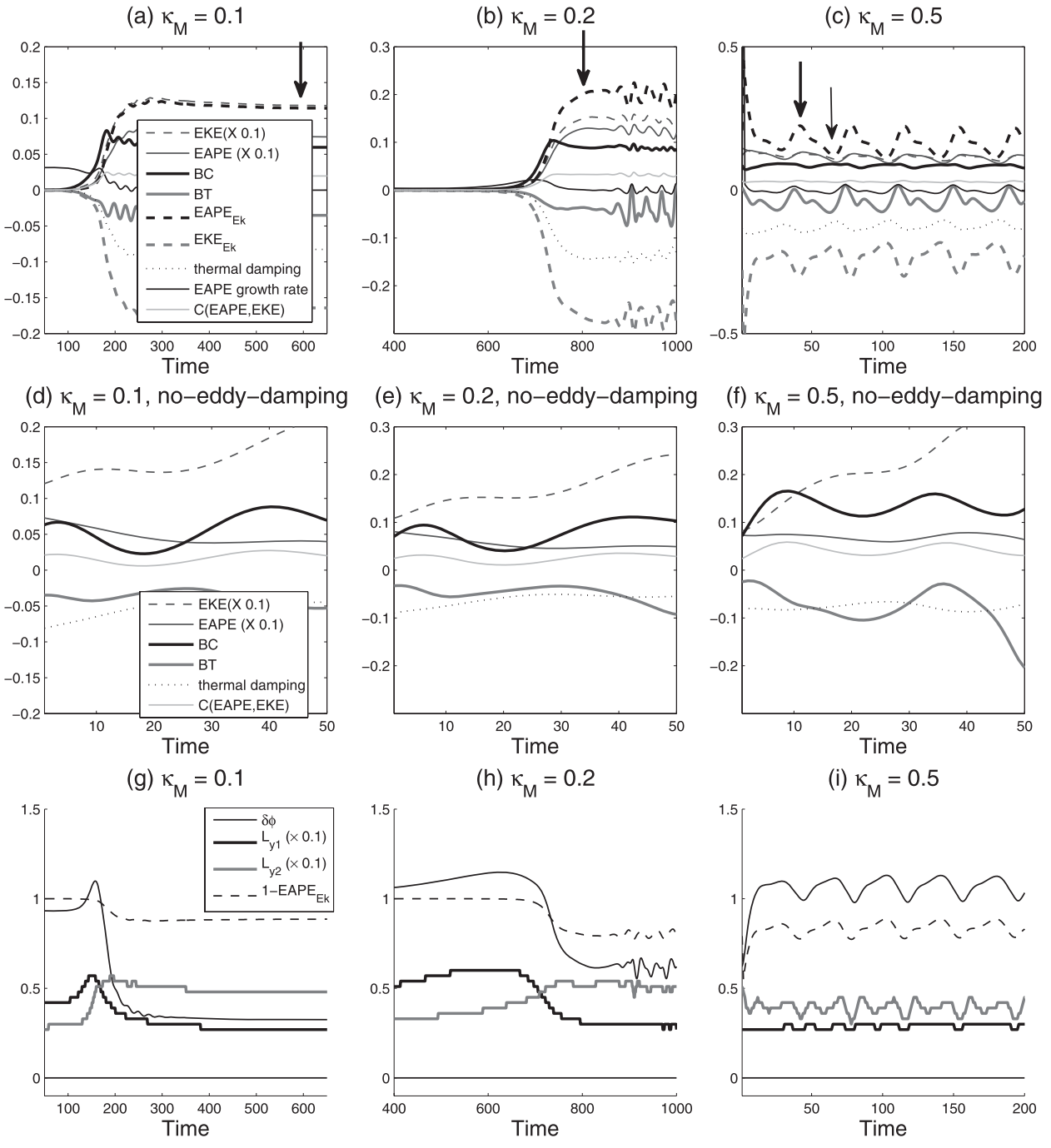

FIG. 4. (a)–(c) The time evolution of EKE, EAPE, baroclinic energy conversion, barotropic energy conversion, EKE_{Ek}, $EAPE_{Ek}$, thermal damping, the instantaneous EAPE growth rate (the EKE growth rate is essentially identical to the EAPE growth and is thus not shown), and C(EAPE, EKE). [See the legend in (a) for $(\kappa_T, \beta) = (1/30, 0.25)$]. Evolution is shown for (a) $\kappa_M = 0.1$, (b) $\kappa_M = 0.2$, and (c) $\kappa_M = 0.5$. The initial condition for the $\kappa_M = 0.5$ case is the day 1000 solution of the $\kappa_M = 0.2$ run. (d)–(f) The first 50-day segment of the model run where the Ekman damping is set to zero in the eddy potential vorticity equation. The initial state is that of (d) day 600 of the run shown in (a),(e) day 800 of (b), and (f) day 40 of (c). These model days are indicated by the thick arrows in (a)–(c). The legend in (a) applies to (b) and (c) and that in (d) applies to (e) and (f). (g)–(i) The time evolution of L_{y1}, L_{y2}, $\delta\phi$, and $1 - EAPE_{Ek}$ for (a),(b), and (c), respectively.

reduction is consistent with the lesser decline of $|\eta|$. This finding indicates that the dissipative energization occurs for all values of κ_M. However, for $\kappa_M = 0.5$, BC never drops below the initial value, indicating that in the regime where TEE decreases with κ_M, BC is more strongly influenced by EKE_{Ek} than by $EAPE_{Ek}$.

5. Conclusions

In this study, we investigated how nonlinear dissipative energization of baroclinic waves occurs in a two-layer model where Ekman damping is applied only to the lower layer. Because the total eddy energy of this system is *always* damped by the Ekman pumping, the nonlinear growth must arise from an enhanced interaction via the Ekman pumping between the eddies and the zonal mean flow. It is found that this growth involves the following process:

1) If the phase difference between the upper- and lower-layer eddies is less than one quarter wavelength, then the lower-layer Ekman pumping can act to produce EAPE ($\mathrm{EAPE_{Ek}} > 0$) while damping the EKE.
2) This EAPE production in turn increases the baroclinic energy conversion (BC) from the ZAPE to the EAPE.

This $\mathrm{BC_{Ek}}$ growth can amplify the baroclinic waves if the net energy production of steps 1 and 2 exceeds the dissipative effect of the Ekman pumping on the EKE. In principle, this mechanism can be tested by comparing baroclinic waves in two parallel calculations, one with and the other without Ekman pumping. However, such a test cannot be performed with a statistically steady state because such a state does not exist if $\kappa_M = 0$. However, transient wave evolutions found in the no-eddy-damping experiments support the above interpretation: the energization occurs because Ekman pumping helps tap ZAPE, and this additional tapping of ZAPE overcompensates for the Ekman damping of EKE. Because the direct effect of the Ekman pumping on the total eddy energy is always dissipative, although not examined in this study, it is reasonable to expect that the same $\mathrm{BC_{Ek}}$ growth process may also operate in the linear dissipative destabilization found by Holopainen (1961), Pedlosky (1983), and Weng and Barcilon (1991).

The relationships between the eddy scale and $\delta\phi$, and between $\delta\phi$ and $\mathrm{EAPE_{Ek}}$, as discussed earlier, imply that eddy scale and $\mathrm{EAPE_{Ek}}$ may also be related to each other. For the three nonzero β cases considered in this study, as can be seen by comparing the eddy scales shown in Figs. 3f–h with the corresponding $\mathrm{EAPE_{Ek}}$ values in Figs. 3b–d, there is a hint that L_{y1} tends to be relatively small when $\mathrm{EAPE_{Ek}}$ is relatively large. Lee (2010) showed that the reduction in $\delta\phi$ (Figs. 4g,h) coincides with jetward movements of upper-layer critical lines and confinement of the upper-layer eddy PV flux toward the jet center. The interpretation of this behavior was that this confinement of the PV flux, in the region where $\partial Q_1/\partial y$ is also large ($\partial Q_1/\partial y$ is maximum at the jet center), favors the occurrence of the inequality in (11). This interpretation can explain the apparent inverse relationship between L_{y1} and $\mathrm{EAPE_{Ek}}$. One implication of this conclusion is that in the presence of surface Ekman pumping, there is a selective generation of small scales in the upper layer. It would be interesting to investigate whether this process can help explain the finding of Rivière et al. (2004) that bottom friction results in significant horizontal scale selection.

Acknowledgments. This study was supported by the National Science Foundation under Grant ATM-0647776. The author acknowledges valuable comments from Steven Feldstein and two anonymous reviewers.

REFERENCES

Bretherton, F. P., 1966: Baroclinic instability and the short wavelength cut-off in terms of potential vorticity. *Quart. J. Roy. Meteor. Soc.,* **92,** 335–345.

Charney, J. G., and A. Eliassen, 1949: A numerical method for predicting the perturbations of the middle latitude westerlies. *Tellus,* **1,** 38–54.

Eady, E. T., 1949: Long waves and cyclone waves. *Tellus,* **1,** 33–52.

Held, I. M., and V. D. Larichev, 1996: Scaling theory for horizontally homogeneous, baroclinically unstable flow on a beta plane. *J. Atmos. Sci.,* **53,** 945–952.

Holopainen, E. O., 1961: On the effect of friction in baroclinic waves. *Tellus,* **13,** 363–367.

Hoskins, B. J., M. E. McIntyre, and A. W. Robertson, 1985: On the use and significance of isentropic potential vorticity maps. *Quart. J. Roy. Meteor. Soc.,* **111,** 877–946.

Hua, B. L., and D. B. Haidvogel, 1986: Numerical simulations of the vertical structure of quasi-geostrophic turbulence. *J. Atmos. Sci.,* **43,** 2923–2936.

James, I. N., 1987: Suppression of baroclinic instability in horizontally sheared flows. *J. Atmos. Sci.,* **44,** 3710–3720.

——, and L. J. Gray, 1986: Concerning the effect of surface drag on the circulation of a baroclinic planetary atmosphere. *Quart. J. Roy. Meteor. Soc.,* **112,** 1231–1250.

Lapeyre, G., and I. M. Held, 2003: Diffusivity, kinetic energy dissipation, and closure theories for the poleward eddy heat flux. *J. Atmos. Sci.,* **60,** 2907–2916.

Lee, S., 2010: Finite-amplitude equilibration of baroclinic waves on a jet. *J. Atmos. Sci.,* **67,** 434–451.

——, and I. M. Held, 1991: Subcritical instability and hysteresis in a two-layer model. *J. Atmos. Sci.,* **48,** 1071–1077.

Lorenz, E. N., 1955: Available potential energy and the maintenance of the general circulation. *Tellus,* **7,** 157–167.

Pedlosky, J., 1970: Finite-amplitude baroclinic waves. *J. Atmos. Sci.,* **27,** 15–30.

——, 1983: The growth and decay of finite-amplitude baroclinic waves. *J. Atmos. Sci.,* **40,** 1863–1876.

Rivière, P., A. M. Treguier, and P. Klein, 2004: Effects of bottom friction on nonlinear equilibration of an oceanic baroclinic jet. *J. Phys. Oceanogr.,* **34,** 416–432.

Robinson, W. A., 2006: On the self-maintenance of midlatitude jets. *J. Atmos. Sci.,* **63,** 2109–2122.

Thompson, A. F., and W. R. Young, 2007: Two-layer baroclinic eddy heat fluxes: Zonal flows and energy balance. *J. Atmos. Sci.,* **64,** 3214–3231.

Weng, H.-Y., and A. Barcilon, 1991: Asymmetric Ekman dissipation, sloping boundaries and linear baroclinic instability. *Geophys. Astrophys. Fluid Dyn.,* **59,** 1–24.